ICAS Paper No. 70-11

REFLECTION OF CURVED SHOCK WAVES

by
S. Mölder
Associate Professor, Department of Mechanical Engineering
McGill University, Montreal, Canada

The Seventh Congress of the International Council of the Aeronautical Sciences

CONSIGLIO NAZIONALE DELLE RICERCHE, ROMA, ITALY / SEPTEMBER 14-18, 1970

Price: 400 Lire

REFLECTION OF CURVED SHOCK WAVES IN STEADY SUPERSONIC FLOW

Sannu Mölder*
McGill University**
Montreal, Canada

Abstract

Numerical results are presented for regular and Mach reflection of curved shock waves at a plane wall. Reflected shock curvature and streamline pressure gradient behind the reflected shock are calculated by imposing zero downstream curvature for the regular reflection, and by matching streamline pressure gradient and curvature at the slip line for Mach reflection. Results show many possible combinations of reflected shock curvature, streamline curvature and pressure gradient. Theoretical arguments and experiments are presented to show that transition from regular to Mach reflection at Mach 2.80 occurs when the Mach stem is normal to the incident flow.

For the region where neither regular nor Mach reflection is possible, a new flow structure is proposed. This structure is compatible with wave reflections between the back of the shock and the sonic line, and the inclination of the sonic line.

I. Introduction

In 1963 Pack (1) wrote a review and critique of shock reflections, considering both unsteady and steady shock waves in ideal gases. Since the writing of this paper Bazhenova et. al. (2) and Glass (3) have experimentally discovered the appearance of a second reflected shock in unsteady Mach interaction, and, on the theoretical side, Henderson (4,5) has published a systematic study of multiple shock confluences. Apart from these two significant developments, the unsolved problems of shock reflection and interaction are as described by Pack. The most stubborn problem of shock reflection was first noted by von Neumann (6) when he observed that regular and Mach reflections persisted for Mach number-shock-strength combinations where neither regular nor Mach reflection solutions existed. The condition is observed at low Mach numbers and for shock angles where the flow behind the incident shock is just supersonic. The problem has been so well-preserved that it has been accorded the title "von Neumann paradox" (Birkhoff (7)). Notable attempts at describing the flow in this paradoxical region are those of Guderley (8) and Sternberg (9). Guderley proposed a three-shock intersection with a Prandtl-Meyer wave emanating from the intersection point; this wave being interposed between the reflected shock and the slip layer. The resulting local patch of supersonic flow has become known as the "Guderley patch". Sternberg suggested that viscosity, in the immediate neighbourhood of the triple point, destroys the validity of the Rankine-Hugonio shock wave relations. The, thus modified, structure of the shock waves, in this non-Rankine-Hugoniot region, can have a considerable influence on the downstream flow. Shindiapin (10) extends the idea of viscosity and heat conduction, acting at a triple point, by use of "short wave" equations, to the calculation of reflected shock angles in the paradoxical region. It is felt that, although there may be regions of Mach (and regular) interaction where the application of non-Rankine-Hugoniot relations becomes a necessity, the possible solutions, with Rankine-Hugoniot type shocks and otherwise inviscid and non-conducting flow, have not yet been fully explored. Part of the discrepancy between theoretical prediction and experiment seems to have been resolved by Smith's (11) measurements where he observed that there is no persistance of regular reflection beyond theoretical limits. Nevertheless, even if we consider this part of the discrepancy resolved, we still have to answer the question: what happens in this paradoxical region?

A question closely related to the above is: How do curved shocks reflect and interact? Crocco (12) first considered the flow behind a single curved shock wave, and pointed to the existance of a shock angle behind which the flow could be straight even though the shock was curved. This angle of the shock wave (which varies with upstream Mach number for shocks in uniform flow) has been called the "Crocco point". Thomas (13) derived an equation relating shock and streamline curvature for two-dimensional flow, and provided numerical results for curved shocks in uniform flow (14). In (15) Thomas provided consistency relations for higher derivatives of shock and streamline curvature, and used these (16) to give the first three approximations to the pressure behind a curved shock on a curved two-dimensional body. Lin and Rubinov (17) used the equations of Thomas (13) to show that for an irrotational upstream flow, a normal shock, at a continuously curving convex wall, is possible only for Mach number above a certain critical value. They also derived a number of interesting relationships for flow behind a single curved shock attached to a curved body.

Shock curvature relations and flow variable gradients behind the shock were derived by Drebinger (18) for both two-dimensional and axisymmetric flow; in both cases under the assumption of a uniform and irrotational freestream. Flow variable gradients were derived also by Gerber and Bartos (19) who then used these to find directions of constant Mach number and constant density contours behind two-dimensional and axisymmetric shock waves.

---

* Associate Professor, Department of Mechanical Engineering.

** This work was performed while the author was on sabbatical leave at the Department of Mechanical Engineering, The University of Sydney.

A homenergic, ideal gas flow with an irrotational upstream has been assumed in all of the above derivations. In this paper, equations for two-dimensional curved shocks will be presented, which allow for a rotational upstream flow. This becomes necessary because the equations are applied to curved reflecting shocks, where the flow behind the curved incident shock is non-uniform and rotational.

For regular reflection of curved shocks at a plane wall we will require the streamline curvature, at the reflection point behind the reflected shock, to be equal to zero. For Mach interactions we will adjust the curvatures of the reflected shock and the Mach stem so that flow curvatures and pressure gradients are matched along the slip line. Presentation of these results is done in their own right as well as to show that the new flow model for the paradoxical region merges smoothly with known flow configurations at the boundaries of the paradoxical region.

The main purpose of this paper is then to derive relations for derivatives of flow variables and use these to explain the observed phenomena of curved intersecting shocks. In particular we examine the processes of transition from regular to Mach reflection and from Mach reflection to a smoothly curving shock wave.

For regular reflection of shocks we consider the whole range of supersonic freestream Mach numbers. Discussion on Mach reflection is limited to Mach 2.80, because a complete set of triple point solutions was available for this Mach number, and also because a wind tunnel was operating at Mach 2.80. However our qualitative conclusions apply from 2.40 on upwards. Conclusions regarding the smooth curving shock again apply to the whole range of supersonic Mach numbers.

II. Theory

In this section we state the basic equations of steady, adiabatic inviscid flow of a calorically and thermally perfect gas. We assume that the flow is two-dimensional and that discontinuities such as shocks and slip layers are infinitesimally thin.

Equations of Motion in Streamline Coordinates (s,n)

The equations of mass, momentum and vorticity can be written, (Hayes and Probstein (20))

$$\frac{\partial \rho q}{\partial s} + \rho q \frac{\partial \delta}{\partial n} = 0 \qquad (1)$$

$$\rho q \frac{\partial q}{\partial s} + \frac{\partial p}{\partial s} = 0 \qquad (2)$$

$$\rho q^2 \frac{\partial \delta}{\partial s} + \frac{\partial p}{\partial n} = 0 \qquad (3)$$

$$\xi = \frac{\partial q}{\partial n} - q \frac{\partial \delta}{\partial s} = \frac{p}{\rho q R} \frac{\partial S}{\partial n} \qquad (4)$$

In the above, q, δ, S are the absolute velocity, the flow deflection angle and the entropy, respectively; ξ is the vorticity, and the distance along and normal to the streamlines are measured by s and n. The flow deflection angle δ is measured positive counter-clockwise from the free-stream direction.

Another useful form of the continuity equation is

$$\frac{M^2 - 1}{\rho q^2} \frac{\partial p}{\partial s} + \frac{\partial \delta}{\partial n} = 0 \qquad (5)$$

The compatibility relations along the C_+ and C_- characteristics are

$$dp \pm \frac{\rho q^2}{\sqrt{M^2 - 1}} d\delta = 0 \qquad (6)$$

where the directions of the characteristics are given by

$$\frac{dn}{ds} = \pm 1/\sqrt{M^2 - 1} \qquad (7)$$

Since the characteristics make an angle $\pm\mu$ with respect to the streamline, we can write,

$$\frac{\partial}{\partial C_+} = \cos\mu \frac{\partial}{\partial s} + \sin\mu \frac{\partial}{\partial n} \qquad (8)$$

$$\frac{\partial}{\partial C_-} = \cos\mu \frac{\partial}{\partial s} - \sin\mu \frac{\partial}{\partial n} \qquad (9)$$

where C_+ and C_- denote distances measured along the C_+ and C_- characteristics and where

$\sin\mu = 1/M$ and $\cos\mu = \sqrt{M^2 - 1}/M$. The strength of the C_- and C_+ characteristics can now be defined as

$$s_- = \frac{\partial p}{\partial C_+} = \frac{\sqrt{M^2 - 1}}{M} \frac{\partial p}{\partial s} + \frac{1}{M} \frac{\partial p}{\partial n} \text{ for } C_- \qquad (10)$$

$$s_+ = \frac{\partial p}{\partial C_-} = \frac{\sqrt{M^2 - 1}}{M} \frac{\partial p}{\partial s} - \frac{1}{M} \frac{\partial p}{\partial n} \text{ for } C_+ \qquad (11)$$

where the strengths are positive and negative for compression and expansion waves, respectively.

Characteristics Strength Ratio

We define the ratio of strengths of the C_+ and C_- characteristics as

$$\lambda_c = \frac{\text{Strength of } C_+ \text{ characteristic}}{\text{Strength of } C_- \text{ characteristic}} = \frac{s_+}{s_-} = \frac{\frac{\partial p}{\partial C_-}}{\frac{\partial p}{\partial C_+}}$$

$$\lambda_c = \frac{s_+}{s_-} = \frac{\sqrt{M^2 - 1}\,\frac{\partial p}{\partial s} - \frac{\partial p}{\partial n}}{\sqrt{M^2 - 1}\,\frac{\partial p}{\partial s} + \frac{\partial p}{\partial n}} \qquad (12)$$

Using Equation (3) to replace $\partial p/\partial n$ in the definition for λ_c, gives

$$\lambda_c = \frac{s_+}{s_-} = \frac{\sqrt{M^2 - 1}\,\frac{\partial p}{\partial s} + \gamma p M^2 \frac{\partial \delta}{\partial s}}{\sqrt{M^2 - 1}\,\frac{\partial p}{\partial s} - \gamma p M^2 \frac{\partial \delta}{\partial s}} \qquad (13)$$

From this we see that λ_c is real only for sonic or supersonic flow. At the supersonic side of a sonic line $\lambda_c = -1$. This implies that a sonic line reflects compressions as expansions and vice versa; but always with unchanged absolute strength.

At a plane wall or line of symmetry $\partial\delta/\partial s = 0$ and $\lambda_c = +1$. For the surface of a free jet, with constant external pressure, $\partial p/\partial s = 0$ and $\lambda_c = -1$. For the flow immediately behind a curved shock it is convenient to consider normal components of characteristic strengths. The characteristics strength ratio is then multiplied by $\sin(\mu - \delta + \theta)/\sin(\mu + \delta - \theta)$ and called the reflection coefficient (Chernyi (21))

$$\lambda = \frac{\sin(\mu - \delta + \theta)}{\sin(\mu + \delta - \theta)}\,\lambda_c \qquad (14)$$

It can be calculated using Equations (14), (22) and (23). The reflection coefficient can be either positive or negative. For uniform irrotational upstream conditions the value of λ behind a curved shock depends on upstream Mach number and shock angle only. This variation is shown in Figure 2. Behind the shock, on the immediate supersonic side of the sonic line, λ is always negative.

We note here that as a general rule if there is communication between surfaces by characteristics which reflect back-and-forth, then the reflection coefficients for the surfaces must have the same sign. In stating this we assume that there are no discontinuities in the region bounded by the surfaces.

The above implies that it is possible for characteristics to reflect between a sonic line and a constant pressure surface, a sonic line and the back of a shock (in the immediate vicinity of the shock), and between a constant pressure surface and the back side of a shock in the immediate vicinity of the sonic point.

Orientation of the Sonic Line

For isoenergetic flow the angle between the streamline and the sonic line can be written, Hayes and Probstein (20),

$$\tan\omega = -\frac{\partial q/\partial s}{\partial q/\partial n} = \frac{\frac{1}{\rho q}\frac{\partial p}{\partial s}}{\xi + q\frac{\partial \delta}{\partial s}} \qquad (15)$$

For the case of conditions immediately behind a two-dimensional shock wave this becomes,

$$\tan\omega = -\frac{\tan^3(\theta_* - \delta_*)\left[3(\gamma+1)\tan^2(\theta_*-\delta_*)+5-\gamma\right]}{\left[1 - \tan^2(\theta_*-\delta_*)\right]\left[(\gamma+1)\tan^2(\theta_*-\delta_*)+2\right]} \qquad (16)$$

where the subscript * pertains to values of shock angle and flow deflection at sonic conditions. A plot of this, obtained from Gerber and Bartos (19), is shown in Figure 1. We note that $\omega = 90^\circ$ at $M_\infty = 1$ and 1.691. The latter Mach number is found from Equation (16) by setting the first term of the denominator equal to zero,

$$\tan^2(\theta_* - \delta_*) = 1 \qquad (17)$$

giving $\theta_* - \delta_* = 45^\circ$ or 135°

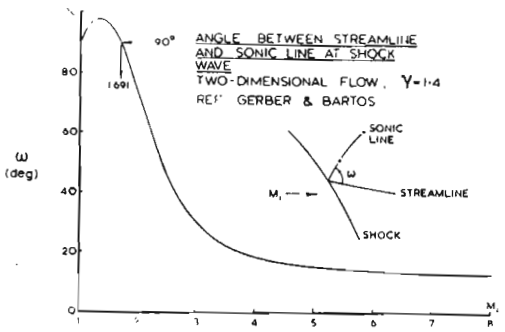

FIGURE 1 - ANGLE BETWEEN SONIC LINE AND STREAMLINE BEHIND TWO-DIMENSIONAL SHOCK WAVE

It is interesting to note that at $M_\infty = 1.691$ the streamline and the sonic line are at right angles, with each making an angle of 45° with the shock wave. Although, as seen from Equation (17), the Mach number at which this occurs depends on γ, the relationship between the angles is independent of γ. At the sonic line the characteristics are perpendicular to the streamlines, since the Mach angle at M=1 is 90°. This means that for a freestream Mach number of 1.691 the characteristics are parallel to the sonic line at the shock. Thus, characteristics reflect between the shock and the sonic line for concave

shocks below $M_\infty = 1.691$ and for convex shocks above $M_\infty = 1.691$. In both cases this is permitted by λ being negative for both the sonic line and the shock in the neighbourhood of their intersection. An implication of this is that it is possible for a sonic line to emanate from the rear of a progressively weakening shock wave. Similarly, for a concave shock, below $M_\infty = 1.691$, communication between the sonic line and the shock is possible since both have negative λ's and the angle between the sonic line and the shock is such that repeated reflection of characteristics is possible. The above arguments will be used later to establish a flow structure which provides a qualitative explanation of flows behind smooth concave shocks with continuous curvature.

Curved Shocks in Non-Uniform Flow

In this section we write the equations for vorticity, streamline curvature and streamline pressure gradient behind a two-dimensional curved shock, which advances into an upstream with finite vorticity, streamline curvature and pressure gradient. Thomas (13) first derived these equations for the simplified case of a uniform upstream state (no curvature and pressure gradient) and a two-dimensional curved shock. Lin and Rubinov (17) gave the equations for a two-dimensional shock with upstream flow curvature and pressure gradient but zero vocticity and Drebinger (18) derived the case for a uniform upstream, but axisymmetric flow.

In our case we intend to apply our relations to a curved reflected shock which lies behind a curved incident shock wave; so that it becomes important to account for flow curvature, pressure gradient and vorticity produced by the incident shock.

Our discussion and derivations are restricted to flow with planar symmetry; for axisymmetric flow the relationships would contain a term which includes the distance from the axis of symmetry. The equations relating shock curvature $\partial\theta/\partial\sigma$ and upstream vorticity ξ_1 to the streamline pressure gradient $\partial p/\partial s$ and streamline curvature $\partial\delta/\partial s$ in front of and behind the shock are derived in the Appendix:

$$E_1\frac{\xi_1}{q_1} + \frac{A_1}{\rho_1 q_1^2}\left(-\frac{\partial p}{\partial s}\right)_1 + B_1\left(\frac{\partial \delta}{\partial s}\right)_1 = \frac{A_2}{\rho_1 q_1^2}\left(-\frac{\partial p}{\partial s}\right)_2 + B_2\left(\frac{\partial \delta}{\partial s}\right)_2 + C\left(\frac{\partial \theta}{\partial \sigma}\right)_1 \qquad (18)$$

$$E_1'\frac{\xi_1}{q_1} + \frac{A_1'}{\rho_1 q_1^2}\left(-\frac{\partial p}{\partial s}\right)_1 + B_1'\left(\frac{\partial \delta}{\partial s}\right)_1 = \frac{A_2'}{\rho_1 q_1^2}\left(-\frac{\partial p}{\partial s}\right)_2 + B_2'\left(\frac{\partial \delta}{\partial s}\right)_2 + C'\left(\frac{\partial \theta}{\partial \sigma}\right)_1 \qquad (19)$$

In these equations the coefficients are independent of the derivatives and are functions of only the freestream Mach number M_1, shock angle θ and ratio of specific heats γ. The functional forms of the coefficients are given in the Appendix.

Solving for the downstream pressure gradient and flow curvature from Equations (18) and (19) gives,

$$\frac{1}{\rho_1 q_1^2}\left(\frac{\partial p}{\partial s}\right)_2 = \frac{\begin{vmatrix} B_2, & -A_1\left(\frac{\partial p}{\partial s}\right)_1/\rho_1 q_1^2 + B_1\left(\frac{\partial \delta}{\partial s}\right)_1 - C\left(\frac{\partial \theta}{\partial \sigma}\right)_1 + E_1\frac{\xi_1}{q_1} \\ B_2', & -A_1'\left(\frac{\partial p}{\partial s}\right)_1/\rho_1 q_1^2 + B_1'\left(\frac{\partial \delta}{\partial s}\right)_1 - C'\left(\frac{\partial \theta}{\partial \sigma}\right)_1 + E_1'\frac{\xi_1}{q_1} \end{vmatrix}}{D_1} \qquad (20)$$

$$\left(\frac{\partial \delta}{\partial s}\right)_2 = \frac{\begin{vmatrix} A_2, & -A_1\left(\frac{\partial p}{\partial s}\right)_1/\rho_1 q_1^2 + B_1\left(\frac{\partial \delta}{\partial s}\right)_1 - C\left(\frac{\partial \theta}{\partial \sigma}\right)_1 + E_1\frac{\xi_1}{q_1} \\ A_2', & -A_1'\left(\frac{\partial p}{\partial s}\right)_1/\rho_1 q_1^2 + B_1'\left(\frac{\partial \delta}{\partial s}\right)_1 - C'\left(\frac{\partial \theta}{\partial \sigma}\right)_1 + E_1'\frac{\xi_1}{q_1} \end{vmatrix}}{D_1} \qquad (21)$$

where $D_1 = \begin{vmatrix} B_2 & -A_2 \\ B_2' & -A_2' \end{vmatrix}$

If the vorticity is produced by a curved shock, with curvature $(\partial\theta/\partial\sigma)_0$, then we can write, Hayes and Probstein (20),

$$\xi_1 = -q_0\frac{\left[1 - \frac{\rho_0}{\rho_1}\right]^2}{\frac{\rho_0}{\rho_1}}\cos\theta_0\left(\frac{\partial \theta}{\partial \sigma}\right)_0 \qquad (22)$$

In the above q_0 is the velocity upstream of the vorticity-producing shock, θ_0 is the shock angle and $(\partial\theta/\partial\sigma)_0$ the shock curvature.

Using Equations (20) and (21) we are now in a position to calculate the pressure gradient and streamline curvature behind curved two-dimensional shocks for various states of upstream flow.

Curved Shocks in Uniform Irrotational Upstream Flow

Uniform flow implies that both $(\partial p/\partial s)_1$ and $(\partial\delta/\partial s)_1$ are zero and irrotational flow requires that $\xi_1 = 0$. This case pertains to the most usual situation encountered with forward shocks

on projectiles advancing into still air. Equations (20) and (21) then become

$$\frac{1}{\rho_1 q_1^2}\left(\frac{\partial p}{\partial s}\right)_2 = \frac{\begin{vmatrix} B_2 & -C \\ B_2' & -C' \end{vmatrix}}{D_1}\left(\frac{\partial \theta}{\partial \sigma}\right)_1 \qquad (23)$$

$$\left(\frac{\partial \delta}{\partial s}\right)_2 = \frac{\begin{vmatrix} A_2 & -C \\ A_2' & -C' \end{vmatrix}}{D_1}\left(\frac{\partial \theta}{\partial \sigma}\right)_1 \qquad (24)$$

From these equations it is seen that both the streamline pressure gradient and streamline curvature behind a shock are zero behind a straight shock wave ($\partial\theta/\partial\sigma = 0$). Furthermore, the pressure gradient is zero whenever the determinant in the numerator of Equation (23) is zero. An expansion of this determinant gives

$$\frac{2}{\gamma + 1}\sin 2\theta = \frac{\sin 2\delta}{4\cos^2(\theta - \delta)} \qquad (25)$$

The solution of this equation, for a given value of the freestream Mach number gives the shock angle where $(\partial p/\partial s)_2 = 0$. This point, and the locus of streamline points with a pressure maximum, emanating downstream from this point, are called the isobaric point and the pressure ridge, respectively. The variation of the isobaric point (θ_p) with Mach number is shown in Figure 2, for the present case of uniform irrotational upstream flow.

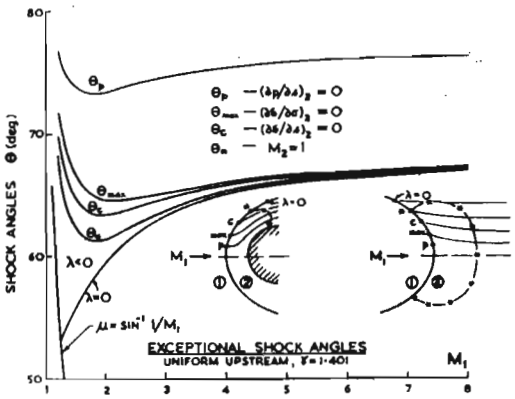

FIGURE 2 - EXCEPTIONAL SHOCK ANGLES FOR TWO-DIMENSIONAL SHOCKS

In a similar manner, the streamline curvature is zero whenever the numerator in Equation (24) is zero. An expansion for this gives,

$$\frac{2\sin 2\theta}{\gamma + 1}\left[1 + (M_2^2 - 2)\sin^2(\theta - \delta)\right] = \frac{\sin 2\delta}{2} \qquad (26)$$

and a solution of this equation for a given M_∞ determines the Crocco-point at which $(\partial\delta/\partial s)_2 = 0$. Analogously, the locus of points downstream of the shock where $(\partial\delta/\partial s)_2 = 0$, which is in fact the inflection point of the streamlines, we will refer to as the Crocco line. For uniform irrotational upstream flow the Crocco-point (θ_c) is shown in Figure 2, and it is noticed that the Crocco-point lies between the sonic point and the point of maximum streamline deflection for all freestream Mach numbers. Note here that the location of the isobaric and Crocco-points does not depend on the shock curvature when the freestream is uniform and irrotational. The existance and significance of these points has been discussed by Crocco (12) and Thomas (14).

III. Regular Reflection of Curved Shocks at a Plane Wall

The reflection of shocks at a plane wall, or the equivalent case of interaction of two equal strength shocks is one of the more elementary problems of shock dynamics. As long as the upstream Mach number is high and the incident shock is weak the readily calculable regular reflection appears. However, if the incident shock reaches above a certain strength (determined by the upstream Mach number) then the reflected shock is no longer able to return the flow to the freestream direction, and regular reflection is no longer possible. We will demonstrate later that transition from regular to Mach reflection occurs before this limiting condition imposed by the reflected shock. We wish to calculate flow properties and their derivatives as well as shock curvatures in the immediate vicinity of the shock interaction point, in the first instance, for the case of regular reflection. We presume γ to be constant throughout, and begin by specifying a Mach number in front of the incident shock M_1, a shock angle θ_1 and a shock curvature $(\partial\theta/\partial\sigma)_1$. On applying the condition that the reflected shock returns the flow to the freestream direction we can immediately calculate the reflected shock properties. Similarly from the incident shock curvature $(\partial\theta/\partial\sigma)_1$, we can, by using Equations (23) and (24), calculate the pressure gradient and streamline curvature behind the incident shock and the vorticity ξ_2 from Equation (22). We now use Equations (20) and (21) for regions in front of and behind the reflected shock, by advancing all variable subscripts by one; first calculating $(\partial\theta/\partial\sigma)_2$ from (21) by imposing the condition $(\partial\delta/\partial s)_3 = 0$, and then finding $(\partial p/\partial s)_3$ from Equation (20). The reflected shock curvature is shown in Figure 3, normalized with respect to the incident shock curvature, and plotted versus the incident shock pressure ratio p_2/p_1. On reflection, weak shocks at high Mach number curve in the opposite sense whereas strong shocks at high Mach number and shocks at low Mach number curve in the same sense. Above a freestream Mach number of 1.6 there is always a given incident

shock strength, for every freestream Mach number, for which the reflected shock is straight. High values of reflected shock curvature are reached when the reflected shock begins to detach. The pressure gradient along the wall

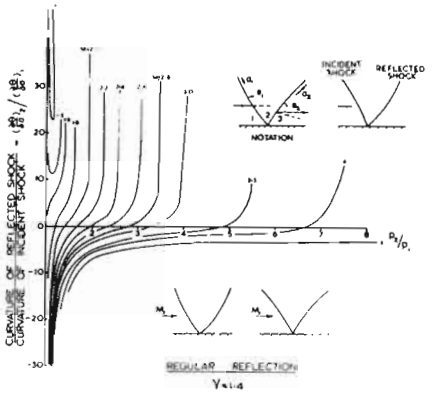

FIGURE 3 - RATIO BETWEEN CURVATURES OF REFLECTED AND INCIDENT SHOCKS FOR REGULAR REFLECTION

behind the reflected shock is shown in Figure 4. It has been normalized with respect to the incident shock curvature and the freestream dynamic pressure. The gradient has the

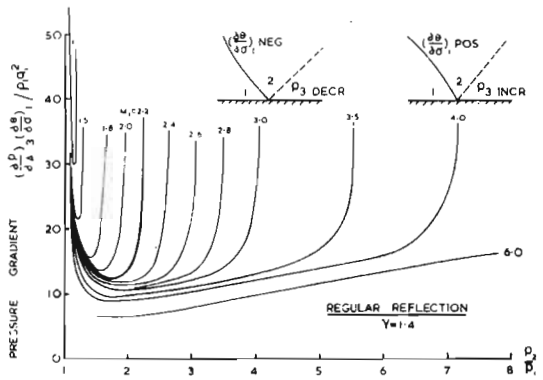

FIGURE 4 - PRESSURE GRADIENT BEHIND REFLECTED SHOCK FOR REGULAR REFLECTION

same sign as the incident shock curvature. High values of shock curvature ratio and pressure gradient should not be viewed as high values of reflected shock curvature and actual pressure gradient but rather as the incident shock curvature tending to zero. This is clearly the case when the incident shock becomes very weak, tending towards a Mach wave at $p_2/p_1 \to 1$. For then, for the case of a uniform freestream, the curvature of the Mach wave $(\partial\theta/\partial\sigma)_1 \to 0$, causing a seeming singularity as $p_2/p_1 \to 1$.

IV. Mach Reflection of Curved Shocks

Flow variables around the triple point confluence were calculated by the method described by Henderson (4). Results for Mach numbers and wave angles are presented in Figures 5a,b and 6 for a freestream Mach number of 2.80. From 5a we see that as we increase the incident shock strength (p_2/p_1) the Mach number behind the incident shock (M_2) decreases to reach a value of one at $p_2/p_1 = 7.14$. However, Mach interaction

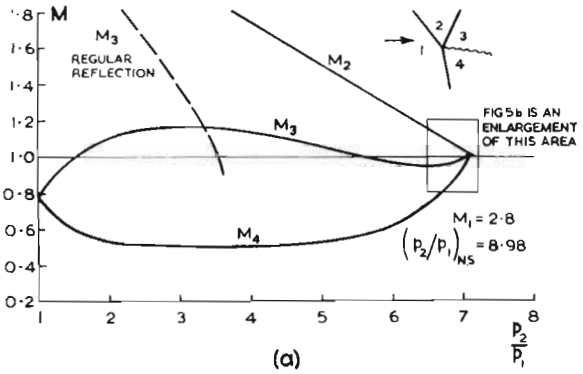

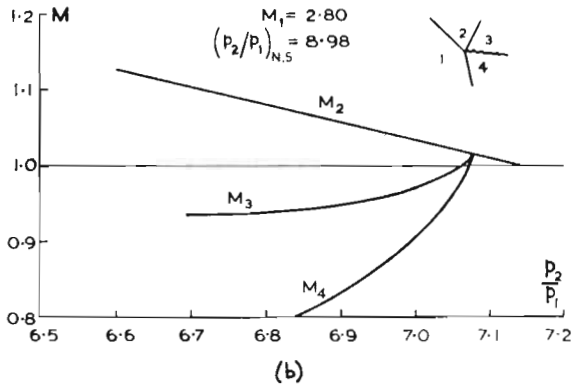

FIGURE 5 - VARIATION OF MACH NUMBERS WITH INCIDENT SHOCK STRENGTH AROUND THREE-SHOCK CONFLUENCE (MACH INTERACTION)

ceases before this, at $p_2/p_1 = 7.074$. At this point both M_3 and M_4 become supersonic and equal to $M_2 = 1.012$. Beyond this point the reflected shock decays to a Mach wave and the incident and Mach shocks become continuous. At this upper limit of Mach interaction the value of $\lambda = 0$; so that, from Figure 2, we conclude that Mach interaction is impossible above the line $\lambda = 0$ and further, since the $\lambda = 0$ line meets the Mach angle curve at $M_1 = 1.245$ we conclude (as has been done previously by others) that Mach interaction is not possible below this

Mach number. We have also shown in Figure 5a the Mach number behind the reflected shock for regular reflection for $M_1 = 2.80$, and it is seen that, although the upper limit of regular reflection lies at $p_2/p_1 = 3.6$, the Mach numbers for regular and Mach reflection are equal at $p_2/p_1 = 3.35$. If one postulates the transition

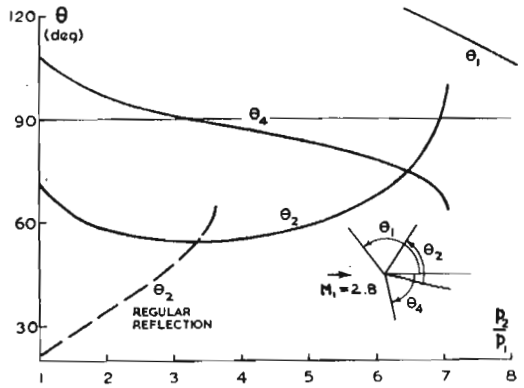

FIGURE 6 - VARIATION OF SHOCK ANGLES WITH INCIDENT SHOCK STRENGTH AROUND THREE-SHOCK CONFLUENCE (MACH INTERACTION)

between regular and Mach reflection to be smooth, then the point of transition would be at $p_2/p_1 = 3.35$ rather than at the upper limit of regular reflection at 3.6. The shock angles are shown in Figure 6. The values of θ_2 for regular and Mach reflection are again equal at $p_2/p_1 = 3.35$, so that again a smooth transition is predicted at this point. Furthermore, we find that $\theta_4 = 90^\circ$ at 3.35 which implies that if transition from regular to Mach reflection begins by the growth of a very small Mach stem then this small stem can grow from the wall (or centerline of symmetry) because flow behind the stem is parallel to the wall.

Just as with regular reflection we make use of Equations (23) and (24) to calculate pressure gradient and streamline curvature in region (2) (having specified the shock curvature $(\partial\theta/\partial\sigma)_1 = 1.0$); and then we calculate the curvature of the reflected and Mach shocks by equating the streamline curvatures and pressure gradient in regions (3) and (4). In doing this we use Equations (23) and (24) for region (4) and Equations (20) and (21) and (22) for region (3). The resulting reflected-to-incident shock curvature ratio $(\partial\theta/\partial\sigma)_2/(\partial\theta/\partial\sigma)_1$ and the Mach shock-to-incident curvature ratio $(\partial\theta/\partial\sigma)_4/(\partial\theta/\partial\sigma)_1$ are shown in Figure 7. In both cases the curvatures have been non-dimensionalized with respect to the incident shock curvature $(\partial\theta/\partial\sigma)_1$. The four singularities at $p_2/p_1 = 1.0$, 3.08, 6.65 and 7.074 should be regarded as places where it is possible for the incident shock to be straight, with finite curvature values of the reflected and Mach shock, rather than places of infinite curvature of the latter. At $p_2/p_1 = 3.95$ and 6.45 it is possible

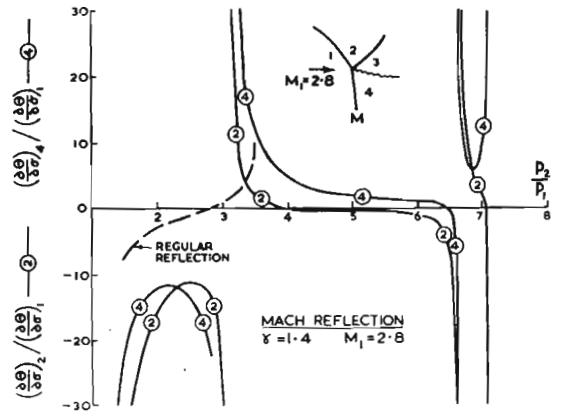

FIGURE 7 - RATIOS BETWEEN CURVATURES OF REFLECTED AND INCIDENT —(2)—, AND MACH AND INCIDENT —(4)— SHOCK WAVES FOR THREE-SHOCK CONFLUENCE

for the reflected and Mach shocks to be straight. The dashed curve for the regular reflected shock crosses its Mach reflection counterpart at $p_2/p_1 = 3.35$, indicating that if transition from regular to Mach interaction occurs at $p_2/p_1 = 3.35$ then the reflected shock curvature changes smoothly. The pressure gradient along the slip layer and the slip layer curvature are shown in Figure 8. The streamline curvature is zero at $p_2/p_1 = 3.35$ as for regular reflection, and the pressure gradients are equal as well. At $p_2/p_1 = 6.45$ the slip line pressure gradient and curvature are both zero. This is due to the Mach stem being straight at this point. Division of the streamline curvature by the incident shock curvature $(\partial\theta/\partial\sigma)_1$, being zero at $p_2/p_1 = 6.65$,

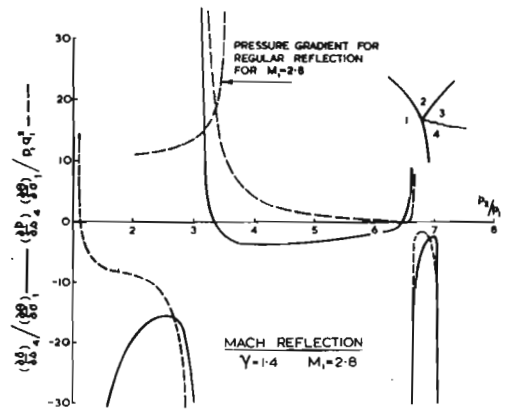

FIGURE 8 - CURVATURE (————) OF, AND PRESSURE GRADIENT (— — — — —) ALONG THE SLIP LAYER BEHIND THE THREE-SHOCK CONFLUENCE

induces a singularity at that point. No such

difficulty arises with the pressure gradient term since it is multiplied by $(\partial\theta/\partial\sigma)_1$. Summarizing the previous discussion, we state that if we assume the transition from regular to Mach reflection to be smooth then (for Mach 2.80) transition would occur at $p_2/p_1 = 3.35$. At this point the Mach stem is normal to the freestream flow. Further we have seen that incident shock, reflected shock, and Mach stem are straight at $p_2/p_1 = 6.65$, 3.95 and 6.45 respectively. Transition between Mach interaction and a smooth curved shock should occur at $p_2/p_1 = 7.074$; this being the point where the reflected shock decays to a Mach wave and the reflection coefficient behind the smooth shock becomes zero. The flow behind the smooth curved shock is described in the next section.

V. Smooth Curved Shocks

Consider now what happens if the incident shock strength is made greater than the maximum for Mach interaction. For $M_1 = 2.80$ this would imply $p_2/p_1 > 7.074$ in Figure 5a, or $\theta > 62.84^\circ$ in Figure 6. The Mach number behind the incident shock M_2 would still be supersonic, the reflected shock would have decayed to a Mach wave and the reflection coefficient would lie in the range $-1 \leq \lambda_c \leq 0$. The flow would appear as shown in Figure 9, with the incident shock and the Mach stem forming one continuous shock wave. A patch of smooth supersonic flow is contained between the sonic line and the shock wave. The latter has a point of inflection between the two sonic points. At this inflection point $(\partial\theta/\partial\sigma)_1 = 0$,

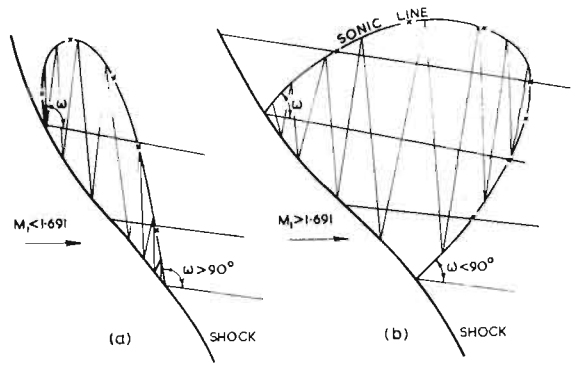

FIGURE 9 - TRANSONIC FLOW BEHIND SMOOTH CURVED SHOCK. (SHOCK ANGLE IN THE RANGE $\theta_{\lambda=0} \leq \theta \leq \theta_*$)

and from Equations (23) and (24) we conclude that $(\partial p/\partial s)_2 = (\partial\delta/\partial s)_2 = 0$ and from (10) and (11) that the strength of the C_- and C_+ characteristics are both zero at the shock inflection point. According to Figure 1 the sonic line makes an angle greater or smaller than 90° to the streamline as M_1 is smaller or larger that 1.691. This leads to the two Figures 9a, 9b. As the shock strength is increased beyond $p_2/p_1 = 7.14$ the Mach number behind the smooth shock becomes <1, and the supersonic patch disappears entirely. Further increases of shock strength will eventually lead to the normal shock at $p_2/p_1 = 8.98$.

VI. Experimental Evidence

Two circular cylinders (¼ in. diameter, 2¼ in. long) were placed parallel to each other in a Mach 2.80 wind tunnel. For two runs the distance between the cylinders was so adjusted that the interacting shock strengths would bracket the transition from regular to Mach reflection. The measured shock angles at the point of intersection were 37.75° and 38.75°. These correspond to $p_2/p_1 = 3.26$ and 3.41 which bracket the theoretically predicted value of 3.35. From Figures 10a and 10b we observe that transition has indeed taken place. The shock angle and pressure ratio for the "detachment" of the regularly reflecting shock are 39° and 3.6; these both being outside the experimentally observed range of transition.

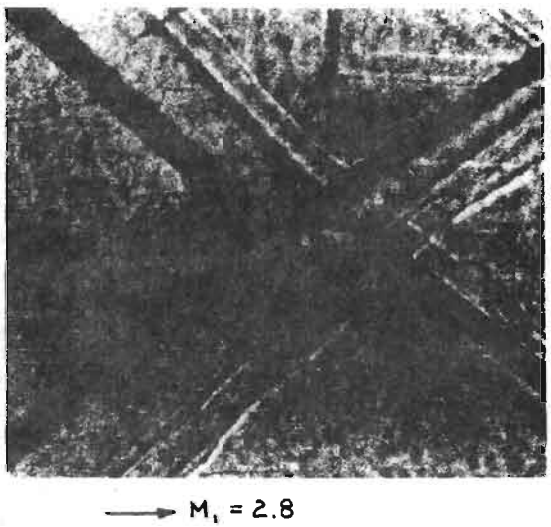

FIGURE 10a - REGULAR REFLECTION NEAR ONSET OF MACH REFLECTION

An attempt was made to establish the transition between Mach interaction and the smooth shock. Larger cylinders (½ in. diameter, 1½ in. long) were moved together until the reflected shock disappeared. Despite the larger cylinders the incident shock was too highly curved to enable an accurate measurement of its angle. Figure 11 shows a very weak and highly curved reflected shock. The incident and Mach shocks are almost continuous.

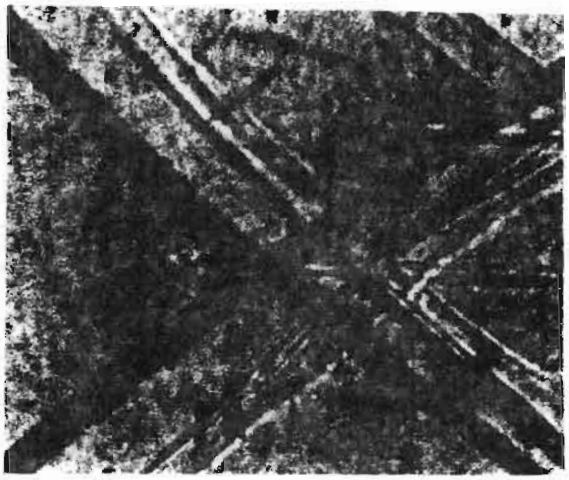

FIGURE 10b - MACH REFLECTION JUST AFTER ONSET

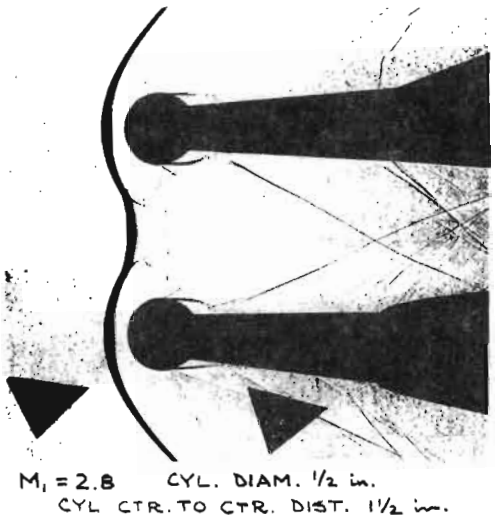

FIGURE 11 - UPPER LIMIT OF MACH REFLECTION, JUST BEFORE DISAPPEARANCE OF REFLECTED SHOCK

VII. Conclusions

Equations of compatibility are derived for first derivatives across curved shock waves in flow with planar symmetry. This has been done where the flow is curved, has a pressure gradient, and is rotational. The equations show that for a uniform irrotational upstream a straight shock always produces a uniform irrotational downstream flow. For a curved shock in uniform flow exceptional points are found, where, behind the shock, the pressure gradient is zero, the flow is straight and no finite strength wave reflection is possible.

The compatibility equations, when applied to regular reflection of oblique shocks, show that below a freestream Mach number of 1.6 the sign of the reflected shock is the same as the sign of the incident shock. Above 1.6, if the incident shock is strong, the shocks are curved in the same sense, but if the incident shock is weak, then they are curved oppositely. Weak incident shocks have small curvature. Strong reflected shocks have large curvature. The pressure gradient on the wall, behind the point of regular reflection, has the same sign as the incident shock curvature. The pressure gradient becomes very large when the reflected shock nears its maximum strength.

For Mach interaction, at Mach 2.8, the zero curvature points occur at the following incident shock strengths p_2/p_1: incident shock - 1.0, 3.05, 6.65, 7.074; reflected shock - 3.95, 7.05; Mach shock - 6.45. The slip layer behind the triple point is straight for p_2/p_1 = 3.35 and 6.45. Pressure is constant along the slip layer for p_2/p_1 = 1.12, 6.45 and 6.55.

At Mach 2.8, a smooth transition from regular to Mach reflection is possible only at p_2/p_1 = 3.35. Experiments confirm transition at this pressure ratio.

Above p_2/p_1 = 7.074 Mach interaction is no longer possible. A smooth supersonic patch is postulated for the range of incident shock strengths 7.074 to 7.140. The patch is bounded by a shock with an inflection point and a sonic line. Two characteristically different supersonic patches appear above and below a freestream Mach number of 1.691.

Smooth transition from Mach interaction to flow with the supersonic patch occurs at p_2/p_1 = 7.074 when the reflected shock becomes a Mach wave. This is confirmed by an independent calculation, using the compatibility relations, which show that the reflection coefficient becomes zero at 7.074.

Acknowledgement

The enthusiastic support of Mr. J.A. Stacey, in performing all the numerical work, is greatly appreciated. Dr. L.F. Henderson provided advice and encouragement. Mr. A. Lozzi conducted the windtunnel tests. Models were made by Mr. A.J. Laws.

The Department of Mechanical Engineering and its head, Professor D.W. George, is thanked for making possible a most pleasant year of sabbatical leave in Sydney.

Appendix

Derivation of Equations of Compatability for First Derivatives of Flow variables across a Curved Shock

Equations relating derivatives of flow variables in front of and behind a curved shock wave are derived from three basic sets of equations: a) partial differential equations of conservation of mass, momentum and energy relating gradients of flow properties at points of continuous flow in front of, or behind, the shock; b) the Rankine-Hugoniot equations relating flow variables immediately in front of and behind the shock; c) geometric relations between derivatives along the shock direction and along and normal to the streamlines. The derivation outlined here follows along the lines of Lin and Rubinov (17), except we here include a term which accounts for vorticity in front of the shock wave. The method will be to take derivatives of the Rankine-Hugoniot equations along the shock direction σ; to relate these derivatives, through geometric relations, to flow variable gradients along and normal to the streamline, and finally to eliminate some of these gradients by using the continuum flow equations. First the Rankine-Hugoniot equations are written as

$$\rho_1 q_1 \sin\theta = \rho_2 q_2 \sin(\theta-\delta) \qquad A1$$

$$p_1 + \rho_1 q_1^2 \sin^2\theta = p_2 + \rho_2 q_2^2 \sin^2(\theta-\delta) \qquad A2$$

$$q_1 \cos\theta = q_2 \cos(\theta-\delta) \qquad A3$$

$$q_1 q_2 \sin\theta \sin(\theta-\delta) = a_*^2 - \frac{\gamma-1}{\gamma+1} q_1^2 \cos^2\theta \qquad A4$$

where q is the velocity and δ is the deflection angle of the flow through the shock ($\delta = \delta_2 - \delta_1$). The subscripts 1, 2 and * refer to conditions before and after the shock and to the point where the Mach number is one. From these we find

$$p_2 = p_1 + \rho_1 \left[q_1 \left(1 - \frac{2}{\gamma+1}\cos^2\theta\right) - a_*^2 \right] \qquad A5$$

$$\text{or } p_2 = p_1 + \rho_1 q_1^2 \left[\sin^2\theta - \tfrac{1}{2}\sin 2\theta \tan(\theta-\delta)\right] \qquad A6$$

$$\text{and } \rho_2 q_2^2 / \rho_1 q_1^2 = \sin 2\theta / \sin 2(\theta-\delta) \qquad A7$$

Secondly we write the geometric relations, relating derivatives along the shock (wrt. σ), to derivatives along and normal to the streamline direction. For a typical variable, say the pressure p, we can write for the derivatives upstream of the shock

$$\left(\frac{\partial p}{\partial \sigma}\right)_1 = \left(\frac{\partial p}{\partial n}\right)_1 \sin\theta + \left(\frac{\partial p}{\partial s}\right)_1 \cos\theta \qquad A8$$

and downstream,

$$\left(\frac{\partial p}{\partial \sigma}\right)_2 = \left(\frac{\partial p}{\partial n}\right)_2 \sin(\theta-\delta) + \left(\frac{\partial p}{\partial s}\right)_2 \cos(\theta-\delta). \qquad A9$$

Using the equations of motion,

$$q\frac{\partial q}{\partial s} = -\frac{1}{\rho}\frac{\partial p}{\partial s} \qquad A10$$

$$\rho q \frac{\partial \delta}{\partial s} = -\frac{\partial p}{\partial n} \qquad A11$$

$$\frac{1-M^2}{q}\frac{\partial q}{\partial s} = -\frac{\partial \delta}{\partial n} \qquad A12$$

with the definition of vorticity,

$$\xi = \frac{\partial q}{\partial n} - q\frac{\partial \delta}{\partial s}$$

and the energy equation in the form

$$\frac{\partial p}{\partial n} = M^2 \rho \left(-\frac{\partial \delta}{\partial s} + \frac{\gamma-1}{q}\xi \right) \qquad A13$$

we can eliminate derivatives in a direction normal to the streamlines from equations A8 and A9.

$$\left(\frac{\partial p}{\partial \sigma}\right)_1 = -\rho_1 q_1^2 \left(\frac{\partial \delta}{\partial s}\right)_1 \sin\theta + \left(\frac{\partial p}{\partial s}\right)_1 \cos\theta \qquad A14$$

$$\left(\frac{\partial p}{\partial \sigma}\right)_2 = -\frac{\sin 2\theta}{2\cos(\theta-\delta)}\left(\frac{\partial \delta}{\partial s}\right)_2 + \frac{1}{\rho_1 q_1^2}\cos(\theta-\delta)\left(\frac{\partial p}{\partial s}\right)_2 \qquad A15$$

We obtain similar expressions for $(\partial\delta/\partial\sigma)_{1,2}$ and $(\partial\rho/\partial\sigma)_{1,2}$.

Differentiating A6 with respect to distance along the shock (σ):

$$\frac{1}{\rho_1 q_1^2}\left(\frac{\partial p}{\partial \sigma}\right)_2 = -\left(\frac{\partial \delta}{\partial s}\right)_1 \sin\theta + \left(\frac{\partial p}{\partial s}\right)_1 \cos\theta + \frac{1}{\rho_1}\left(\frac{\partial \rho}{\partial \sigma}\right)_1 b - \frac{a_*^2}{q}$$

$$+ \frac{2}{q_1}\left(\frac{\partial q}{\partial \sigma}\right) b + \frac{2}{\gamma+1}\sin 2\theta \left(\frac{\partial \theta}{\partial \sigma} - \left(\frac{\partial \delta}{\partial \sigma}\right)_1 \right) \qquad A16$$

where $b = 1 + (2/(\gamma+1))\cos^2\theta$

$c = (2/(\gamma+1))\sin 2\theta$

$\frac{\partial \theta}{\partial \sigma}$ is the shock curvature

Using A14 and similar equations for δ, ρ and q to eliminate the σ - derivatives from A16, we can equate $(\partial p/\partial\sigma)_2$ in A15 and A16, to obtain an equation of the form

$$\left(-\frac{\partial p}{\partial s}\right)_1 \frac{A_1}{\rho_1 q_1^2} + \left(\frac{\partial \delta}{\partial s}\right)_1 B_1 + \frac{\xi_1}{q_1} E_1 = \left(-\frac{\partial p}{\partial s}\right)_2 \frac{A_2}{\rho_1 q_1^2} + \left(\frac{\partial \delta}{\partial s}\right)_2 B_2 + \frac{\partial \theta}{\partial \sigma} C \qquad A17$$

where the coefficients are

$$A_1 = (2/(\gamma+1))\cos\theta(1-\gamma)/2 + (3M_1^2-4)\sin^2\theta)$$

$$B_1 = (2/(\gamma+1))\sin\theta((M_1^2-4)\sin^2\theta + (5-\gamma)/2)$$

$$E_1 = -(2/(\gamma+1))\sin^3\theta((\gamma-1)M_1^2+2) \qquad \text{A18}$$

$$A_2 = \cos(\theta-\delta)$$

$$B_2 = \sin2\theta/2\cos(\theta-\delta)$$

$$C = (2/\gamma+1)\sin2\theta$$

A similar treatment of equation A6 yields the following equation:

$$\left(-\frac{\partial p}{\partial s}\right)_1 \frac{A_1'}{\rho_1 q_1^2} + \left(\frac{\partial \delta}{\partial s}\right)_1 B_1' + \frac{\xi_1}{q_1} E_1' = \left(-\frac{\partial p}{\partial s}\right)_2 \frac{A_2'}{\rho_1 q_1^2} + \left(\frac{\partial \delta}{\partial s}\right)_2 B_2' + \frac{\partial \theta}{\partial \sigma} C' \qquad \text{A19}$$

where the coefficients are

$$A_2' = 1 + (M_2^2-2)\sin^2(\theta-\delta)$$

$$B_2' = \sin2\theta$$

$$C' = \sin2\delta/2\cos(\theta-\delta)$$

$$A_1' = M_1^2\cos^2\theta\cos\delta - (M_1^2-1)\cos(2\theta+\delta) \qquad \text{A20}$$

$$B_1' = M_1^2\sin^2\theta\sin\delta + \sin(2\theta+\delta)$$

$$E_1' = -\sin^2\theta\sin\delta(2 + M_1^2(\gamma-1))$$

These are the required relations of compatibility where equations A17 and A19 can be treated as two equations in any two unknown derivatives. The known derivatives in this case being specified by the boundary conditions of the problem and the coefficients being found by calculating M_2, θ and δ from the oblique shock relations.

References

(1) Pack, D.C. 1963 J. Fluid Mech. 18, 549.

(2) Bazhenova, T.V. et.al., 1968 NASA TT F-585.

(3) Glass, I.I. 1968 UTIAS Progress Report.

(4) Henderson, L.F. 1964 Aero. Quarterly 15, 181.

(5) Henderson, L.F. 1966 Aero. Quarterly 17, 1.

(6) von Neumann, J. 1943 U.S. Navy Buord Rep. 12.

(7) Birkhoff, G. 1950 Hydrodynamics, Princetown Univ. Press.

(8) Guderley, K.G. 1962 The Theory of Transonic Flow, Perg. Press.

(9) Sternberg, J. 1959 Phys. of Fluids 2, 179.

(10) Shindiapin, G. 1969 PMM 33, 368.

(11) Smith, W.R. 1959 Phys. of Fluids 2, 533.

(12) Crocco, L. 1937 Aerotechnica 17, 519.

(13) Thomas, T.Y. 1947 J. Math. Phys. 26. 62.

(14) Thomas, T.Y. 1949 J. Math. Phys. 27, 279.

(15) Thomas, T.Y. 1949 J. Math. Phys. 28, 62.

(16) Thomas, T.Y. 1951 Jour. Math. & Mech. 6, 132.

(17) Lin, C.C., Rubinov, S.I. 1948 J. Math. Phys. 27, 105.

(18) Drebinger, J.W. 1950 Ph.D. Thesis, Arts & Science, Harvard.

(19) Gerber, N., Bartos, J. 1960 Aerospace Sci. 27, 958.

(20) Hayes, W.D., Probstein, R.F. 1966 Hypersonic Flow Theory, Acad. Press.

(21) Chernyi, G.G. 1961 Introduction to Hypersonic Flow, Acad. Press.